16th World Conference on Earthquake, 16WCEE 2017

Santiago Chile, January 9th to 13th 2017

Paper N° 4348

Registration Code: S-G1464455498

EFFECT OF THE 2D SPATIAL VARIABILITY OF LINEAR SOIL PROPERTIES ON THE SPATIAL VARIABILITY OF SURFACE GROUND MOTION

E. El Haber[(1)], D. Abdelmassih[(2)], C. Cornou[(3)], D. Jongmans[(4)], T. Al Bittar[(5)], F. Lopez-Caballero[(6)], N. Salloum[(7)]

[(1)] *Phd Student, ISTerre, elias.el-haber@univ-grenoble-alpes.fr*
[(2)] *Phd, Lebanese University, dalia.abdelmassih@ul.edu.lb*
[(3)] *Phd, ISTerre, cecile.cornou@univ-grenoble-alpes.fr*
[(4)] *Phd, ISTerre, denis.jongmans@univ-grenoble-alpes.fr*
[(5)] *Phd, Lebanese University, tamara.albittar@gmail.com*
[(6)] *Phd, MSSMat, fernando.lopez-caballero@ecp.fr*
[(7)] *Phd, Lebanese University, nancysalloum9@hotmail.com*

Abstract

Spatial variability of earthquake ground motion (SVEGM) refers to the differences in amplitude and phase between recordings of the same earthquake at different locations. SVEGM can have a significant effect on the dynamic response of large structures with large dimensions, such as dams, nuclear power plants, bridges and lifeline facilities. Usually, SVEGM is attributed to the wave passage, spatial incoherence, and local site effects. In the near-surface, geological process (sedimentation, erosion) and anthropogenic activities can lead to small scale spatial heterogeneities of soil mechanical properties. In order to study the effects of such near-surface heterogeneities on the spatial variability of surface ground motion, a set of numerical experiments are designed based on the spatial variability of soil properties (shear-wave velocities *Vs*) measured in the alluvial plain of Beirut, Lebanon. The 2D spatially variable *Vs* are modeled using random field theory and discretized using the EOLE method (Expansion Optimal Linear Estimation). Seismic ground motions were simulated within 1 Hz and 25 Hz using FLAC2D for a plane wave excitation with P-SV polarization. The horizontal autocorrelation distance was taken equal to 5 and 10 m, while the vertical autocorrelation distance was fixed to 2m. The coefficient of variation of *Vs* was fixed to 20% and 40%. Computed surface time series clearly outline locally diffracted surface waves at the ground heterogeneity, which lead to large spatial variation of the surface ground motion in terms of amplification and duration. The frequency-and spatially dependent ground motion parameters (amplification, PGV, Arias Intensity, Arias Duration) in terms of average values and standard deviations were found to be mainly controlled by the coefficient of variation on *Vs* and, less significantly, by the horizontal autocorrelation distance of *Vs*.

Keywords: Spatial variability; Seismic response; Random field; 2D numerical modeling

1. Introduction

Spatial variability of earthquake ground motion (SVEGM) refers to the differences in amplitude and phase between recordings of the same earthquake at different locations. SVEGM can have a significant effect on the dynamic response of large structures with large dimensions, such as dams, nuclear power plants, bridges and lifeline facilities. Usually, SVEGM is attributed to the wave passage, spatial incoherence, and local site effects. In the near-surface, the natural processes of erosion, weathering and deposition and anthropogenic deposits can lead to small scale spatial heterogeneities of soil mechanical properties [e.g. 1, 2].

Characterization of the spatial variability in soil seismic properties are thus of main importance to assess seismic ground motion variability [e.g. 3, 4]. Although widely used in geotechnical engineering, probabilistic modeling approaches that enable to quantify the soil parameters uncertainties related to the spatial variability using random fields [5] have not yet deserved full interest in the seismological community, mainly due to the difficulty in measuring small spatial scale variation of mechanical properties [2, 6]. Although the few 2D probabilistic approaches [3, 4, 7, 8] performed so far have highlighted importance of spatial variability of soil properties on the surface ground motion, the use of different surface ground motion indicators (spectral response, Peak Ground Acceleration, amplification, Housner intensity) and the use (or not) of variability of input ground motion and non-linear soil properties make uneasy a clear understanding of the relative impact of soil properties variability (coefficient of variation, fluctuation spatial scale) on the ground motion.

In this paper, we therefore present a sensitivity study on the effect of the 2D spatial variability of linear soil properties on the spatial variability of surface ground motion, by making use of in-situ measurements in the alluvial plain of Nahr Beirut (Lebanon) which have allowed to quantify random properties of shear-wave velocity at small spatial scale. After modeling the shear-wave velocity spatial variability by random fields, synthetic seismograms are computed using a 2D Finite Difference code. The surface amplification, the spatial variation of Peak Ground Velocity *(PGV)*, the Arias intensity and the Arias duration are then analyzed.

2. Probabilistic analysis and modeling

2.1. Soil data and statistical parameters

The Quaternary alluvial plain of Nahr Beirut (Beirut, Lebanon) was the subject of extensive near-surface geotechnical (borehole measurements, SPT, laboratory measurements) and geophysical (seismic, resistivity) campaigns [6]. These experiments highlighted interbedded layers of pebble, gravel, sand and clay overlaying marly limestone of Tertiary age (fig. (1)) with strong vertical and horizontal variability. From Salloum et al. (2014) [6], a typical soil column has been derived: a gravel layer of 7.5 m thickness with a shear-wave velocity (*Vs*) of 350 m/s overlaying a softer clay layer of 8 m thickness with Vs=150 m/s and a weathered limestone. The coefficient of variation (COV_{Vs}) for *Vs* was found to be 13% and 44% for the clay and gravel layers, respectively [9]. The fluctuation spatial scale of a given soil properties can be given by the autocorrelation distance [10]. While vertical autocorrelation distance, $\theta_{y,}$ is ranging between 0.5 to 2 m in the sedimentary layers, the horizontal autocorrelation distance, θ_x, is ranging between 3.8 and 10.6 m depending on the considered depth.

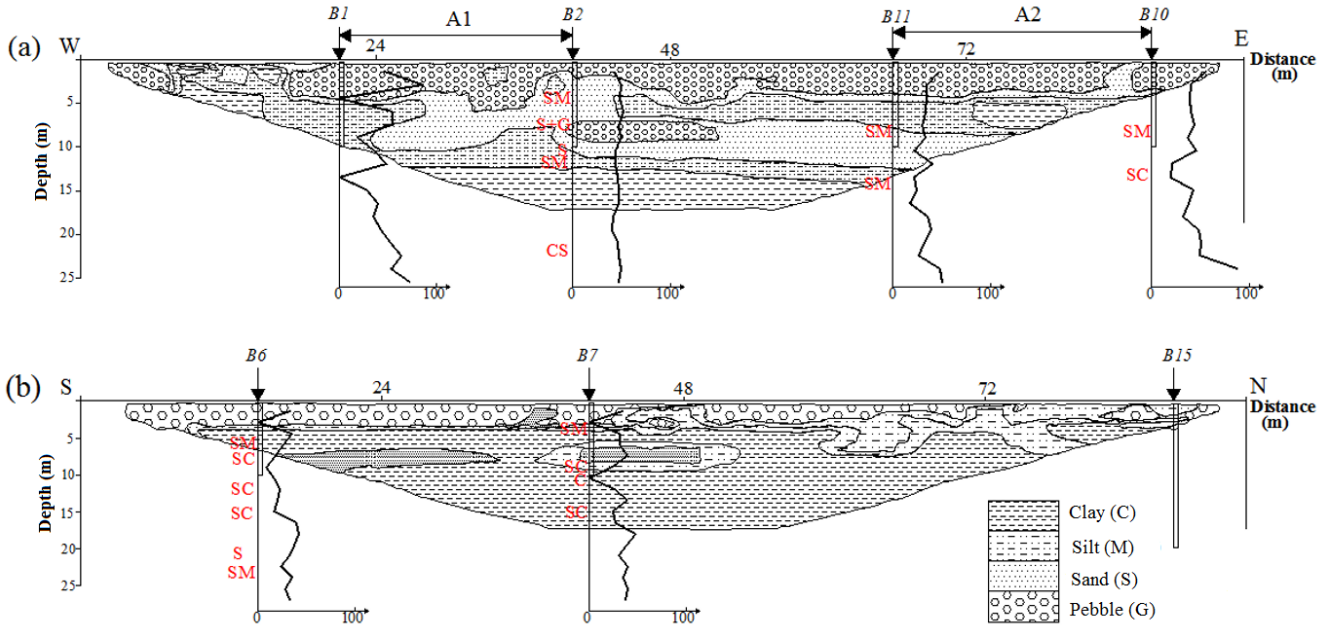

Fig. 1- Example of geological interpretation in the alluvial plain of Nahr-Beirut. In red are shown the seives analysis results: G: Pebbles, S: Sand, M: Limon, C Clay (USCS classification) [9].

In order to study the effect of spatial variations of near-surface shear-wave structure on the surface seismic response, a parametric study was done for a simple case: a sediment layer over a rigid bedrock. The two sedimentary layers mentioned above were thus homogenized in a clayey-gravel unit with an average Vs= 220m/s as indicated in the soil structure used for modeling in Fig.2. While the vertical autocorrelation distance was fixed to 2 m, two values were considered for the horizontal autocorrelation distance, 5 m and 10 m; and $COV_{Vs,}$ 20% and 40%. The 2D soil structure used in the modeling is a 22 m x 165 m model as sketched in Fig 2.

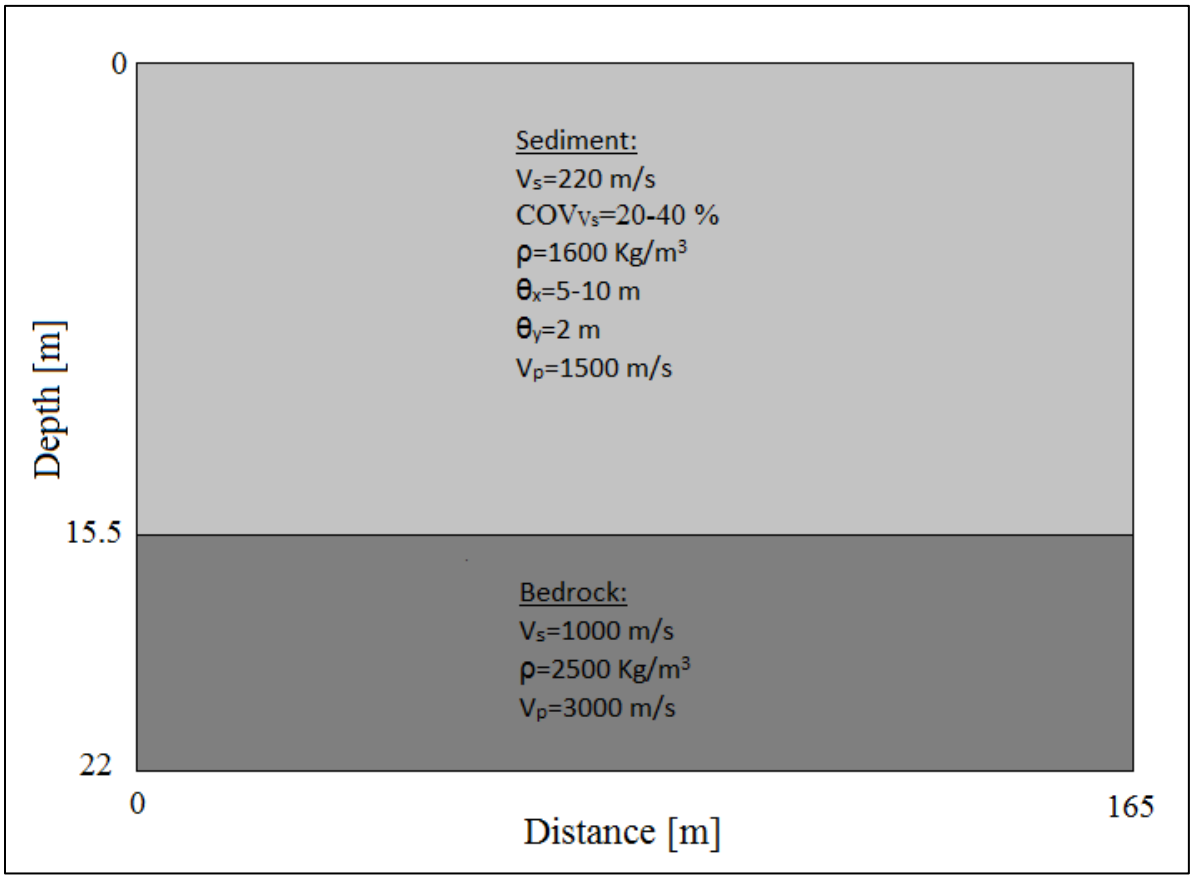

Fig. 2- Schematic of 2D soil structure used for wave propagation modeling and mechanical elastic properties of the homogenized sediment layer of Nahr-Beirut alluvial plain.

2.2. Random Process discretization

In probabilistic seismic modeling, the *Vs* is modeled as a random field. The V_s variability is characterized by a probability distribution (with the mean value (μ_{vs}) and the coefficient of variation (COV_{Vs})), and an autocorrelation function (defined by vertical and horizontal autocorrelation distances (θ_y and θ_x, respectively). Wave propagation modeling is performed for several discretization of the random field. The number of wave propagation modeling (i.e. realizations) should be large enough to ensure convergence of the average value of the output engineering parameters (e.g. Fourier amplitude spectra, Arias Intensity, PGV, …).

The Expansion Optimal Linear Estimation (EOLE) [11] is the method used in our study to discretize the random field. This method is an extension of the Optimal Linear Estimation (OLE) developed by Li and Der Kiureghian (1993) [12] and is based on the kriging method. The dimension of the 2D stochastic domain is defined in both horizontal (X) and vertical (Y) directions. The Monte Carlo method is then applied to generate several random fields' discretization. In the EOLE, the statistical characterization of the random field *Vs* is defined by a squared exponential autocorrelation function given by Eq. (1) and a log-normal probability distribution. Thus, using the EOLE method, V_s at each point of the stochastic domain is estimated from the calculated autocorrelation matrix and its eigen values and vectors.

$$\Omega = \exp\left(-\left[\frac{|k.\Delta h|}{a}\right]^2\right) \quad (1)$$

Where Ω is the correlation coefficient, $k.\Delta h$ is the lag (data interval) distance and a is the autocorrelation distance.

2.3. FLAC^{2D} modeling

In our study, the commercial software FLAC^{2D} is used to propagate seismic waves in the 2D domain [e.g. 13, 14, 15, 16]. This software is based on the finite difference method.

The mesh size Δl is chosen less than one tenth of the minimum wavelength to avoid numerical dispersion phenomena (Eq. 2) [17].

$$\Delta l_{max} \leq \frac{\lambda_{min}}{10} \leq \frac{Vs_{min}}{10.f_{max}} \quad (2)$$

Where Δl_{max} is the maximum size of the finite difference mesh, λ_{min} is the minimum wave length, Vs_{min} is the minimum shear wave velocity, and f_{max} is the maximum wave frequency.

In all the discretized random fields used in FLAC simulations, the minimum value of Vs was found to be 50 m/s. Since the maximum computed frequency is 25Hz, Δl should be less than 0.2 m as per Eq. (2). The minimum computational frequency is 1 Hz.

In the elastic model used in this study, the necessary parameters are the density ρ, the shear modulus G and the bulk modulus K, which are related to V_S and V_p. Regarding the boundary conditions, zero horizontal displacements are applied along lateral boundaries of the model and the horizontal and vertical movements are fixed at its base. The initial stresses due to the weight of soil are calculated in FLAC^{2D} by applying the gravity acceleration (i.e. 9.81 m/s2) in the negative y-direction. After initialization of the stresses, a seismic shear stress excitation (Eq. (3)) of a plane wave of type SV is applied to the base of the model after releasing the horizontal displacement there. The source time function is a pseudo-Dirac having a flat Fourier amplitude spectrum equals to 1 between 1 and 25 Hz (Fig.3). Free field boundaries are applied to the side edges of the model. A quiet boundary is applied to the model base. In order to model a flexible base that absorbs some of the energy emitted by the waves reflected on the surface and arriving to the model base, the seismic signal is applied as σ_s shear stress at the base of the model.

$$\sigma_s = 2.(\rho.V_s).\upsilon_s \quad (3)$$

Where σ_s is the applied shear stress, ρ is the soil density, V_s is the shear wave velocity of the medium where the signal is applied and υ_s is the horizontal component of the velocity signal.

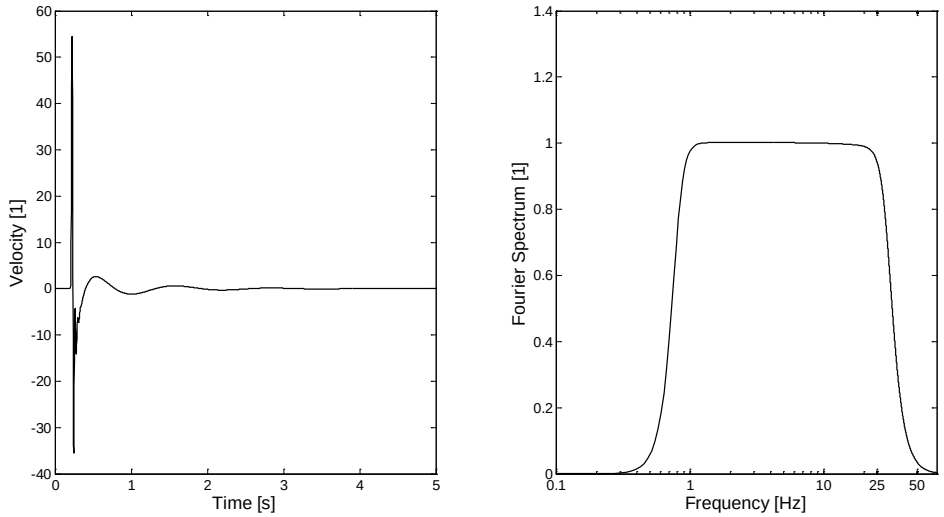

Fig. 3-Incident Signal (left) and Fourier Amplitude Spectrum (right), [1] refers to no unit.

2.4. Example of a shear wave velocity realization and ground motion modeling

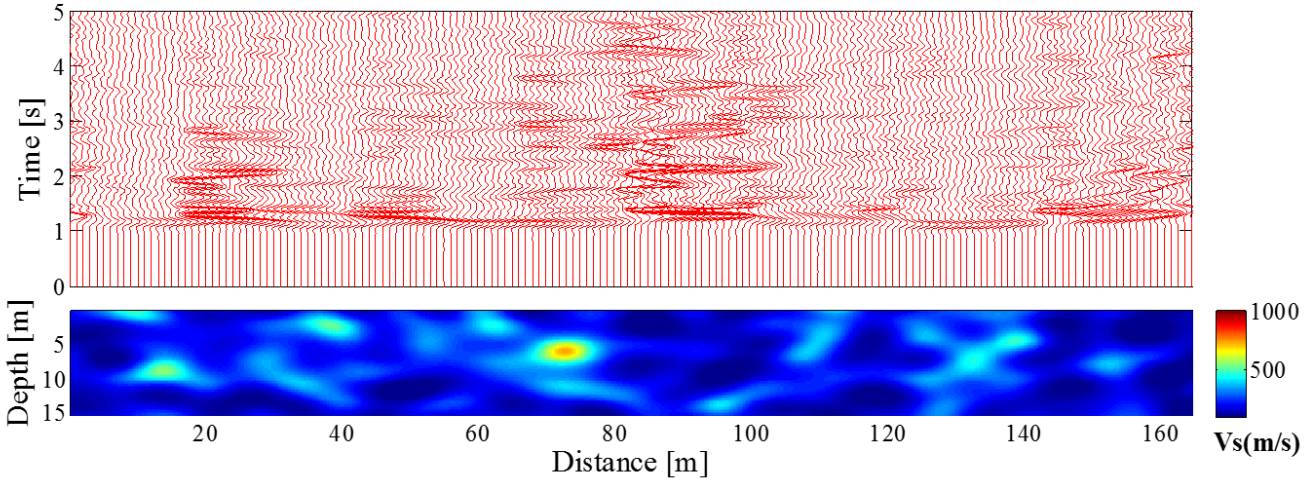

Fig. 4-Bottom: random field of *Vs, values of Vs being indicated in the colorbar*. Top: synthetic velocities computed for the *V*s random field.

Fig.4 (top) displays the seismograms (velocities) at the surface computed for a given realization of the Vs random field for COV_{Vs}=40% and θ_x=5m (Fig. 4 (bottom)). For surface receivers located at about 20 m and between 80 and 100 m, we notice amplification and duration lengthening of ground motion, consistent with the presence of low Vs values surrounded by higher values of Vs in the near surface of the model (Fig. 4 (bottom)) leading to trapping waves effects.

The amplitude of the signals recorded at receivers at the domain boundaries are absorbed due to the absorbent conditions used in FLAC^{2D}. Thus, for accurate calculation of the mean values of the further analyzed engineering parameters, all the edge receivers will be disregarded.

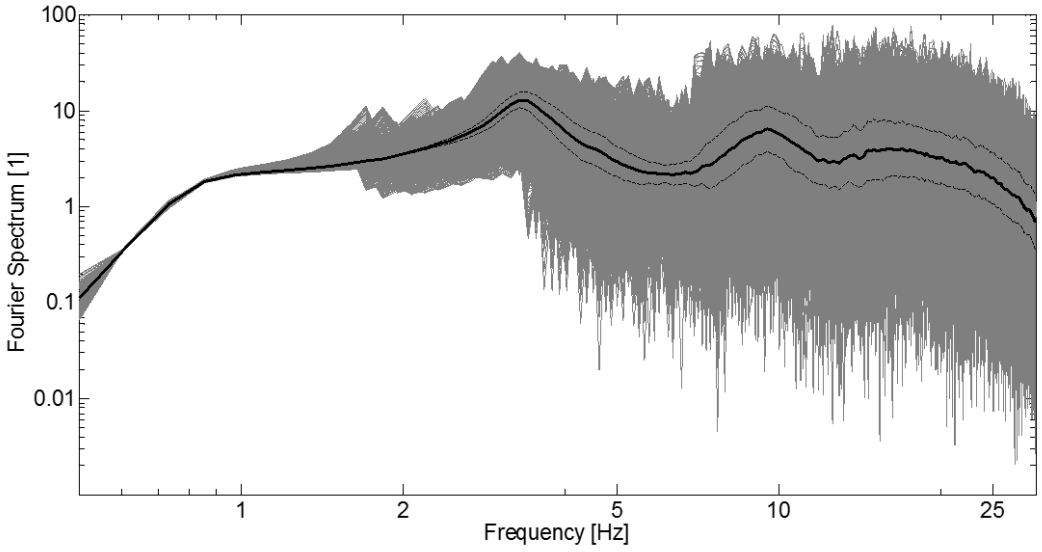

Fig. 5- Fourier amplitude spectrum of all the recordings at the surface for the 100 simulations with COV_{Vs}=40% and θ_x=5m. The black and dashed lines represent the mean (geometric average) and standard deviation, respectively.

In order to test the convergence of the probabilistic modeling, Fourier amplitude spectra (Fig. (5)) computed at all the receivers and considering 100 simulations (realizations) are used. Since the Fourier amplitude spectra

follow a lognormal distribution at each frequency, we computed the average and standard deviation by using the geometric mean and the standard deviation of the natural logarithms of the spectral values.

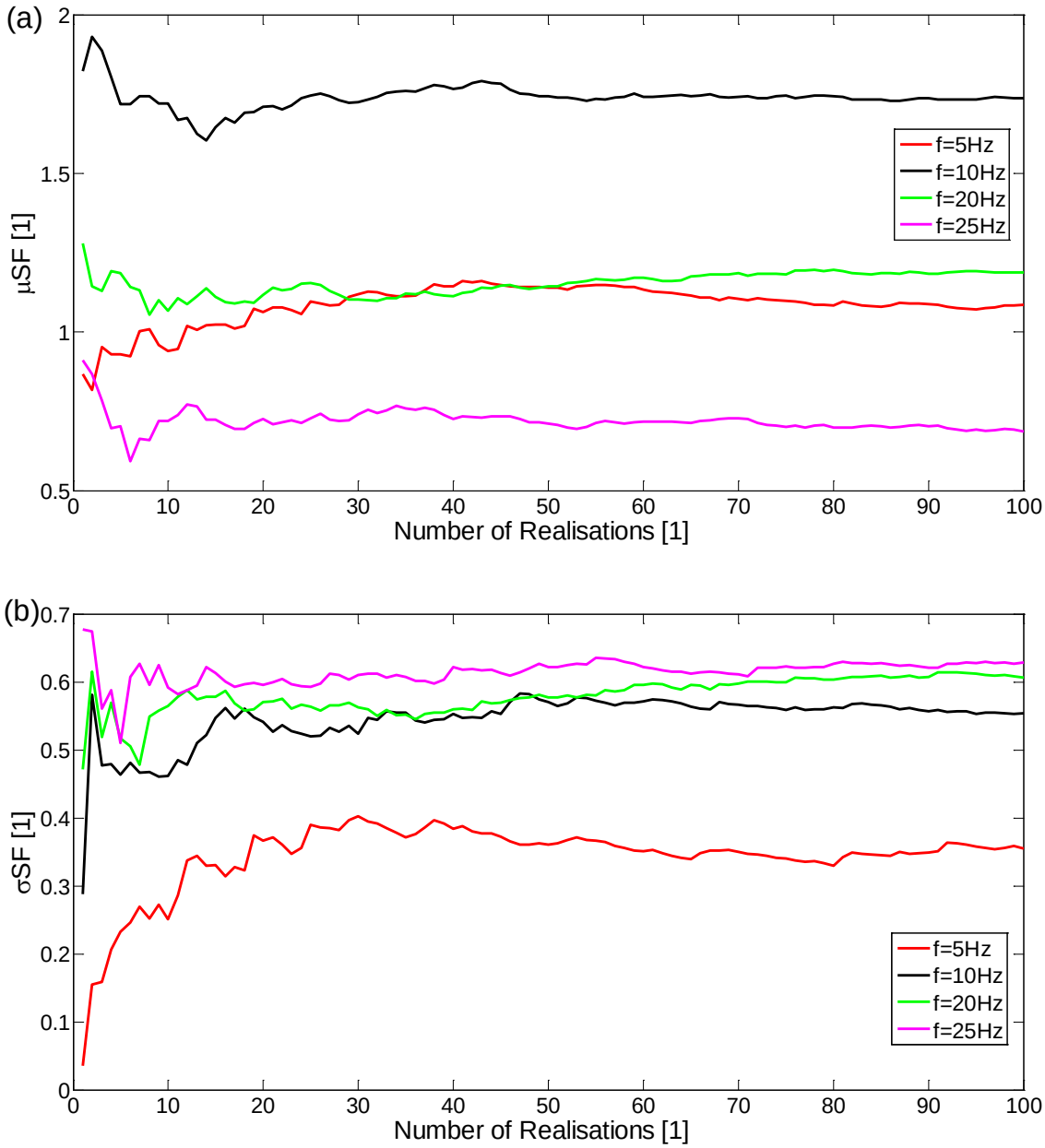

Fig. 6- Variation of the Fourier Spectrum mean (a) and the Fourier Spectrum standard deviation (b) in function of the number of simulations for COV_{Vs} =40% and θ_x=5m.

The obtained average and the standard deviation of the Fourier amplitude spectra are converging to a constant value while increasing the number of realizations (Fig. (6)). Constant values, whatever the frequency considered, are reached after 50 realizations, which indicates that 100 realizations are enough for the convergence of the Fourier amplitude average spectra. Such convergence tests have been performed for all the other cases considered in the parametric study and for all the analyzed parameters (Amplification, Peak Ground Velocity,

Arias Intensity and Duration) that will be presented in the following sections and have all confirmed that 100 realizations lead to stable ground motion parameters averages and standard deviations.

3. Ground motion engineering parameters

3.1. Amplification

The amplification function (*AF*) is the ratio between the Fourier amplitude spectrum of the signal recorded at the surface of the sediment and at outcropping rock.

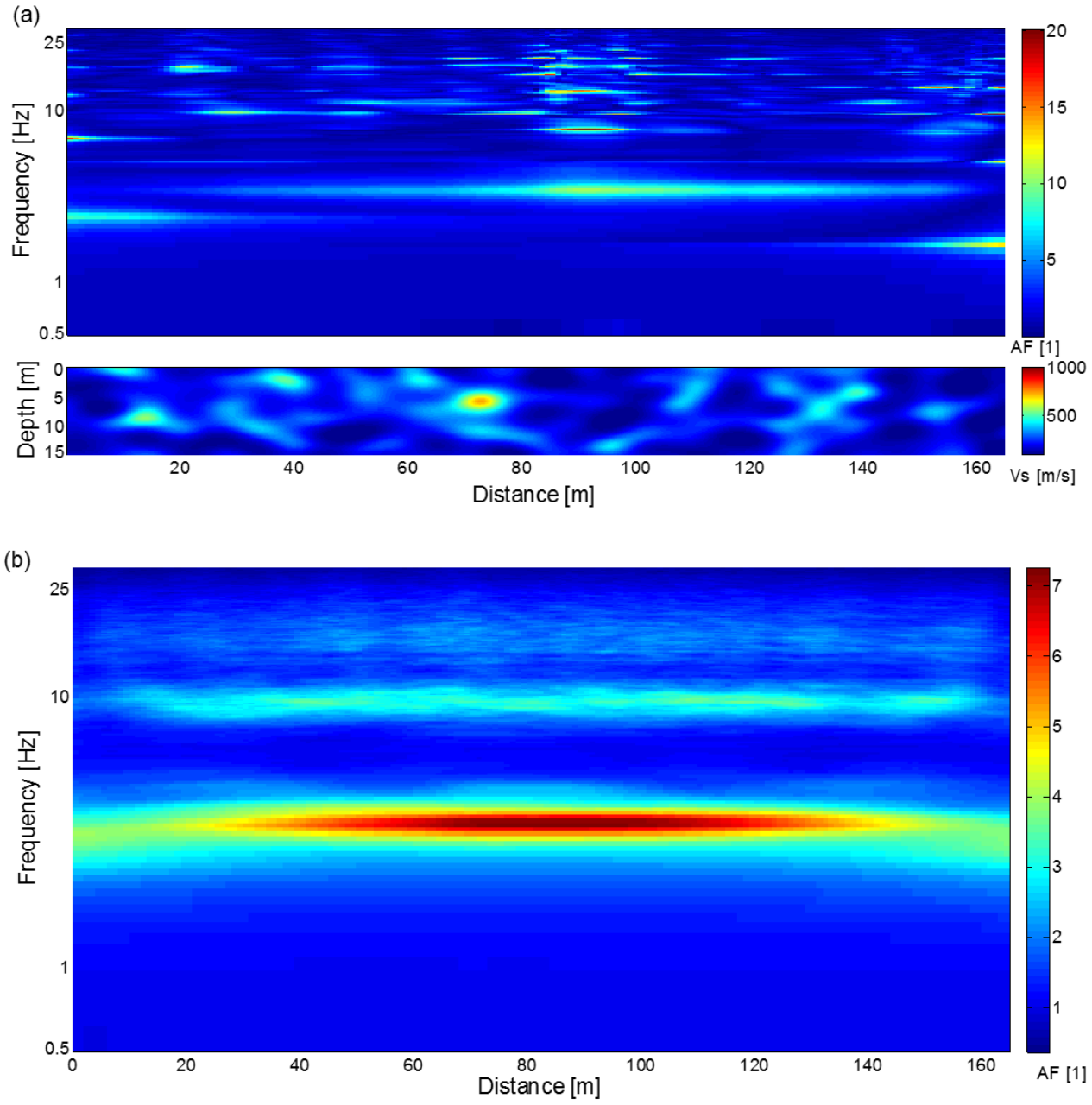

Fig. 7- (a) Bottom: random field of Vs, values of Vs being indicated in the colorbar. Top: Amplification of the Synthetic signals shown in Fig. (4) (b) Spatial variability of the average amplification at surface for different frequencies.

Fig.7 (a) (top) displays the amplification at the surface computed for a given realization of the Vs random field for COV_{Vs}=40% and θ_x=5m (Fig. 7 (a) (bottom)). Similar to Fig. 4, due to the presence of low Vs values surrounded by higher values of Vs in the near surface of the model (Fig. 7 (a) (bottom)), especially between 80 and 100 m, we notice amplification of ground motion.

Fig.7 (b) shows the average amplification for different frequencies at each receptor on surface for COV_{Vs}=40% and θ_x=5m. Again, the results at borders show the effect of the boundary conditions initiated in FLAC^{2D}. An attenuation in the maximum amplification is noted with the increase of the frequency.

In order to compare amplification obtained for the different cases (various COV_{Vs} and θ_{x}), we considered the average amplification at all surface receivers (except the ones affected by the boundary conditions) for the 100 realizations.

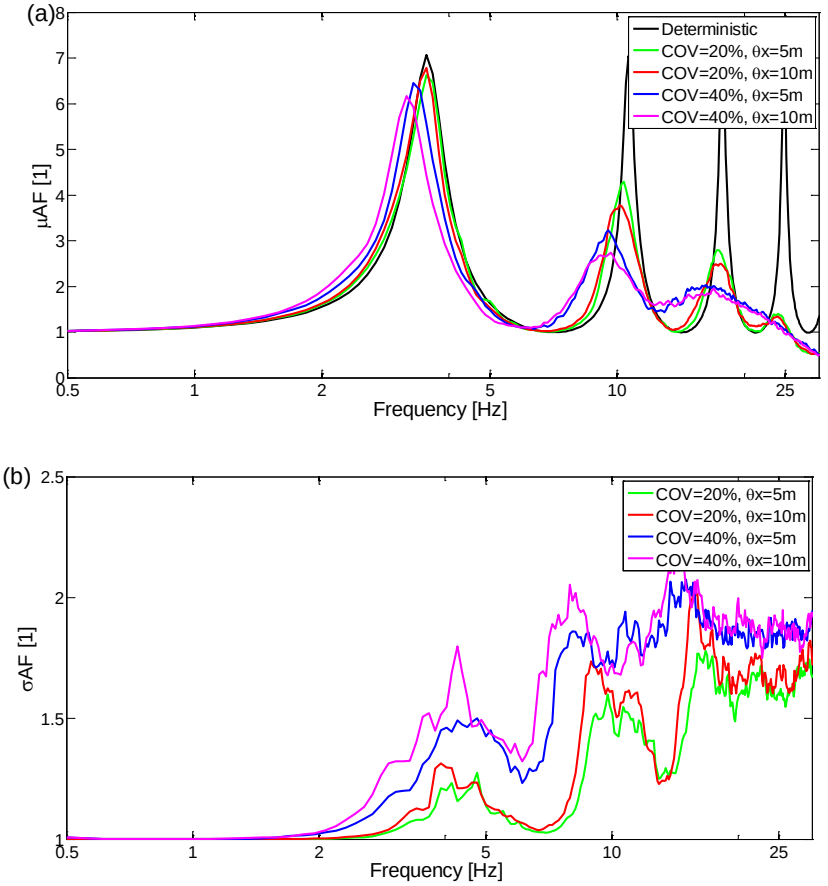

Fig. 8-(a) Average amplification as a function of frequency for five simulations: one deterministic by considering the homogeneous soil profile and four probabilistic with COV_{VS}=20 and 40%, θx=10 m and COV_{VS}=20 and 40%, θx=5 m. (b) Standard variation of the amplification as a function of frequency for the same simulations.

For the 4 combinations of COV_{Vs} and θ_x, the maximum amplification (Fig.8 (a)) is found to be lower than the amplification obtained by the theoretical deterministic 1D SV response considering the homogenized soil profile (Fig. 2). Ground motion amplification is highly decreasing at high frequency, the attenuation increasing with larger values of COV_{Vs} and θ_x. The fundamental frequency also decreases with the increase of COV_{Vs} and θ_x; while the reduction in the maximum amplification and the fundamental frequency is about 10% for COV_{Vs} = 40% and θ_x =10m

The standard deviation, σ_{AF}, of the amplification is displayed in Fig.8 (b). σ_{AF} increases with the increase of COV_{Vs} and θ_x , σ_{AF} being however largely controlled by COV_{Vs} , and reaches a constant value at high frequency,

-

3.2. Spatial variation of Peak Ground Velocity (ΔPGV)

The variation of the Peak Ground Velocity (*ΔPGV*) at a given inter-receivers distance, *d*, is the average of the absolute difference between *PGV* considering all receivers pairs separated by *d*.

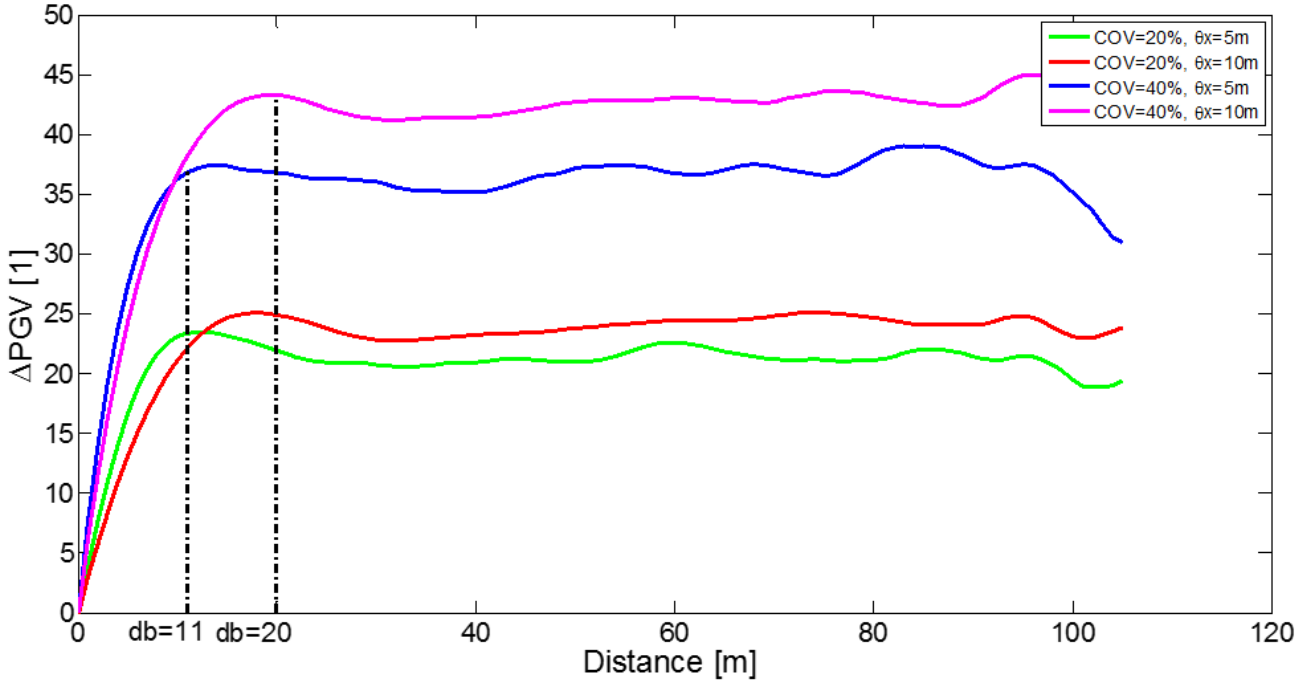

Fig. 9-Spatial variation of the Peak Ground Velocity (*ΔPGV*) as a function of inter-receivers distance (d) for various COV_{VS} *and* θx

Fig.9 displays the spatial variation of *ΔPGV* considering various inter-receivers distances for different COV_{VS} and θx. All curves exhibit the same shape with a first increase of *ΔPGV* with *d* before reaching a constant value. Interestingly, constant *ΔPGV* are reach at break distances (d_b) corresponding to $d_b = 2\theta x$ ($d_b \approx 11$ m for θx =5 m; $d_b \approx 20$ m for θx =10 m) (see Fig. 9). Furthermore, constant *ΔPGV* significantly increases with COV_{VS}.

3.3. Arias Intensity and Duration

The Arias Intensity (*AI*) (Eq. (4)) determines the intensity of shaking [18]. It is defined by the following equation:

$$AI = \frac{\pi}{2g}\int_0^{\infty} a(t)^2 dt \quad (5)$$

Where *a(t)* is the ground acceleration and *g* is the acceleration due to gravity

In this paper, the AI is calculated for the velocities at surface using Eq. (6)

$$AI = \frac{\pi}{2g}\int_0^{\infty} v(t)^2 dt \quad (6)$$

The duration of the Arias Intensity D_{AI} is defined as the difference between the time where 5% of the total energy is reached and the time where 95% of the total energy is reached (Eq. (7)).

$$D_{AI} = t_{E=0.95AI} - t_{E=0.05AI} \quad (7)$$

The values of *AI* and D_{AI} computed for the deterministic case and the four probabilistic cases are plotted and compared in Table 1.

Table 1-Arias Intensity and Duration for the different cases

Simulation	**Deterministic**	**Probabilistic COV_{Vs}=20% θx=5 m**	**Probabilistic COV_{Vs}=20% θx=10 m**	**Probabilistic COV_{Vs}=40% θx=5 m**	**Probabilistic COV_{Vs}=40% θx=10 m**
Arias Intensity *AI*	257.4607	271.7879	270.1071	313.4905	311.4087
Duration D_{AI}	0.7100	0.9386	0.9411	1.5919	1.3608

The increase of spatial variability (COV_{VS} and θ_x) of the soil properties contributes to increase of the Arias intensity and the duration of the signals at the surface. AI and D_{AI} are mainly influenced by COV_{VS}, *AI* increasing by 20 % for COV_{VS} =40%. When COV_{VS} increases, the duration becomes more sensitive to θ_x. Indeed, for COV_{VS} =20%, the duration is almost the same for θ_x =5m and θ_x =10m. When COV_{VS} reaches 40%, the duration for θ_x =5m is 15% larger than the duration for θ_x =10m. For COV_{VS} =40%, the duration obtained by probabilistic approach is larger (almost the double) than the one obtained by deterministic analysis.

4. Conclusion

In order to study the effects of such near-surface heterogeneities on the spatial variability of surface ground motion, a set of numerical experiments are designed based on the spatial variability of soil properties (shear-wave velocities *Vs*) measured in the alluvial plain of Beirut, Lebanon.

In this paper, a parametric study from a simple velocity structure (a sedimentary layer over a half-space) is performed in order to determine the effect of soil fluctuations on the spatial variability of ground motion. Two soil fluctuation parameters are considered in this study: the coefficient of variation on the shear-wave velocity (COV_{Vs}) and the horizontal autocorrelation distance (θ_x) on the *Vs* value. Mechanical elastic average properties and their related variability were derived from past measurements in the Quaternary alluvial plain of Beirut (Lebanon). The effects of these soil parameters fluctuation are studied in terms of amplification, spatial variation of Peak Ground Velocity, Arias intensity and Arias Duration.

Comparing to the deterministic 1D amplification by considering a simple homogenous layer overlaying a halfspace, both amplification and resonance frequency at the fundamental mode decrease in the probabilistic approach, larger decrease being observed for larger COV_{Vs}. While ground motion average amplification is highly attenuated at high frequencies, related standard deviations increase, especially for larger COV_{Vs} and θ_x.

For the other parameters (variation of PGV, Arias Intensity and Arias duration), The duration of the signal is increased by about 20% and 50% for COV_{Vs} of 20% and 40%, respectively, when considering fluctuation of V_s. Interestingly, the spatial variation of PGV increases with COV_{Vs} and θ_x, and reaches a constant value after a distance of 2 θ_x.

Even though the ground motion engineering parameters are found to be sensitive to COV_{Vs} and θ_x, we clearly observed however that the ground motion parameters variation are mainly controlled by COV_{Vs}.

5. Acknowledgements

This work was funded by the Institut de Recherche pour le Développement (IRD), the JEAI – SAMMoVA research unit, ISTerre, the Lebanese University and MSSMat.

6. References

[1] Einsele, G. (2000): Sedimentary basins: evolution, facies, and sediment budget. *Springer.4*.

[2] Pagliaroli, A., Lanzo, G., Tommasi, P., & Di Fiore, V. (2013): Dynamic characterization of soils and soft rocks of the Central Archeological Area of Rome. *Bulletin of earthquake engineering*, 12 (3), 1365-1381.

[3] Thompson, E., Baise, L., Kayen, R., & Guzina, B. (2009): Impediments to Predicting Site Response: Seismic Property Estimation and Modeling Simplifications. *Bulletin of the Seismological Society of America*, BSSA, 99, 2927-2949.

[4] Pagliaroli, A., Moscatelli, M., Raspa, G., & Naso, G. (2014): Seismic microzonation of the central archaeological area of Rome: results and uncertainties. *Bulletin of earthquake engineering*, 12, 1405–1428.

[5] Popescu, R. (1995): Stochastic variability of soil properties: data analysis, digital simulation, effects on system behavior. *Princeton University*.

[6] Salloum, N., Jongmans, D., Cornou,C., Youssef Abdel Massih, D.,HageChehade,F., Voisin, C., and Mariscal, A (2014): The shear wave velocity structure of the heterogeneous alluvial plain of Beirut (Lebanon): Combined analysis of geophysical and geotechnical data. *Geophys. J. Int.*, vol.199, 2014, p.894–913.

[7] Nour, A., Slimani, A., Laouami, N., & Afra, H. (2003): Finite element model for the probabilistic seismic response of heterogeneous soil profile. *Soil dynamics and earthquake engineering*, 23 (5), 331-348.

[8] Assimaki, A., Pecker, A., Popescu, R., & Prevost, J. (2003): Effects of spatial variability of soil properties on surface ground motion. *Journal of earthquake engineering*, 1-44.

[9] Salloum, N. (2015). Evaluation de la variabilité spatiale des paramètres géotechniques du sol à partir de mesures géophysiques: application à la plaine alluviale de Nahr-Beyrouth (Liban). *Phd thesis, Universite Joseph Fourier, Grenoble.*

[10] Vanmarcke, E. (1983): Random fields: analysis & synthesis. *MIT Press. Cambridge*.

[11] Sudret, B., & Der Kiureghian, A. (2000): Stochastic finite element methods and reliability: a state-of-the-art report. *Department of Civil and Environmental Engineering, University of California*.

[12] Li, C.-C., & Der Kiureghian, A. (1993): Optimal discretization of random fields. *Journal of Engineering Mechanics*, 119 (6), 1136-1154.

[13] Bouckovalas, G. D., & Papadimitriou, A. G. (2005): Numerical evaluation of slope topography effects on seismic ground motion. *Soil Dynamics and Earthquake Engineering*, 25 (7), 547-558.

[14] Pagliaroli, A. (2006) : Studio numerico e perimentale dei fenomeni di amplificazione sismica locale di rilievi isolati. Roma. Ph.D. *Thesis, Università di Roma "La Sapienza"*.

[15] Stamatopoulos, C. A., Bassanou, M., Brennan, A. J., & Madabhushi, G. (2007): Mitigation of the seismic motion near the edge of cliff-type topographies. *Soil Dynamics and Earthquake Engineering*, 27 (12), 1082-1100.

[16] Stamatopoulos, C. A., & Bassanou, M. (2009). Mitigation of the seismic motion near the edge of cliff-type topographies using anchors and piles. *Bulletin of Earthquake Engineering*, 71 (1), 221-253.

[17] Bourdeau, C. (2005): Effets de site et mouvements de versant en zones sismiques: apport de la modélisation numérique. *Ph.D thesis. École Nationale Supérieure des Mines de Paris*.

[18] Arias, A. (1970): Measure of earthquake intensity. *Massachusetts Inst. of Tech., Cambridge. Univ. of Chile, Santiago de Chile.*